



Antennas and Reaction Centers of Photosynthetic Bacteria

Structure, Interactions, and Dynamics

Proceedings of an International Workshop
Feldafing, Bavaria, F.R.G., March 23–25, 1985

Editor: M. E. Michel-Beyerle

With 168 Figures

Springer-Verlag
Berlin Heidelberg New York Tokyo

Contents

| | | |
|---|--|----|
| Part I | Antennas: Structure and Energy Transfer | |
| <hr/> | | |
| Structure of Antenna Polypeptides. By H. Zuber | | 2 |
| The Crystal and Molecular Structure of C-Phycocyanin By R. Huber | | 15 |
| C-Phycocyanin from <i>Mastigocladus laminosus</i> . Isolation and Properties of Subunits and Small Aggregates. By W. John, R. Fischer, S. Siebzehrübl, and H. Scheer (With 9 Figures) | | 17 |
| Picosecond Time-Resolved, Polarized Fluorescence Decay of Phycobilisomes and Constituent Biliproteins Isolated from <i>Mastigocladus laminosus</i> By S. Schneider, P. Geiselhart, T. Mindl, F. Dörr, W. John, R. Fischer, and H. Scheer (With 4 Figures) | | 26 |
| Fluorescence Behaviour of Crystallized C-Phycocyanin (Trimer) from <i>Mastigocladus laminosus</i> By S. Schneider, P. Geiselhart, C. Scharnagl, T. Schirmer, W. Bode, W. Sidler, and H. Zuber (With 4 Figures) | | 36 |
| Energy-Transfer Kinetics in Phycobilisomes By A.R. Holzwarth (With 2 Figures) | | 45 |
| Exciton State and Energy Transfer in Bacterial Membranes: The Role of Pigment-Protein Cyclic Unit Structures By R.M. Pearlstein and H. Zuber | | 53 |
| Carotenoid-Bacteriochlorophyll Interactions By R.J. Cogdell (With 1 Figure) | | 62 |
| Bacteriochlorophyll <i>a</i> - and <i>c</i> -Protein Complexes from Chlorosomes of Green Sulfur Bacteria Compared with Bacteriochlorophyll <i>c</i> Aggregates in CH ₂ Cl ₂ -Hexane. By J.M. Olson, P.D. Gerola, G.H. van Brakel, R.F. Meiburg, and H. Vasmel (With 8 Figures) ... | | 67 |
| Reverse-Phase High-Performance Liquid Chromatography of Antenna Pigment- and Chlorosomal Proteins of <i>Chloroflexus</i> <i>aurantiacus</i> . By R. Feick (With 2 Figures) | | 74 |

| | |
|--|----|
| Fluorescence-Detected Magnetic Resonance of the Antenna Bacteriochlorophyll Triplet States of Purple Photosynthetic Bacteria. By A. Angerhofer, J.U. von Schütz, and H.C. Wolf (With 1 Figure) | 78 |
| High-Resolution ^1H NMR of Light-Harvesting Chlorophyll- Proteins. By C. Dijkema, G.F.W. Searle, and T.J. Schaafsma | 81 |
| Crystallization and Linear Dichroism Measurements of the B800- 850 Antenna Pigment-Protein Complex from <i>Rhodopseudomonas</i> <i>sphaeroides</i> 2.4.1 By J.P. Allen, R. Theiler, and G. Feher (With 2 Figures) | 82 |
| Crystallization of the B800-850-complex from <i>Rhodopseudomonas</i> <i>acidophila</i> Strain 7750 By R.J. Cogdell, K. Woolley, R.C. Mackenzie, J.G. Lindsay, H. Michel, J. Dobler, and W. Zinth (With 6 Figures) | 85 |
| Linear Dichroism (LD) and Absorption Spectra of Crystals of B800-850 Light-Harvesting Complexes of <i>Rhodopseudomonas</i> <i>capsulata</i> . By W. Mäntele, K. Steck, T. Wacker, W. Welte, B. Levoir, and J. Breton (With 5 Figures) | 88 |

Part II Reaction Centers: Structure and Interactions

| | |
|--|-----|
| The Crystal Structure of the Photosynthetic Reaction Center from <i>Rhodopseudomonas viridis</i> By J. Deisenhofer and H. Michel (With 2 Figures) | 94 |
| Single Crystals from Reaction Centers of <i>Rhodopseudomonas viridis</i> Studied by Polarized Light. By W. Zinth, M. Sander, J. Dobler, W. Kaiser, and H. Michel (With 3 Figures) | 97 |
| On the Analysis of Optical Spectra of <i>Rhodopseudomonas viridis</i> Reaction Centers By E.W. Knapp and S.F. Fischer (With 3 Figures) | 103 |
| Orientation of the Chromophores in the Reaction Center of <i>Rhodopseudomonas viridis</i> . Comparison of Low-Temperature Linear Dichroism Spectra with a Model Derived from X-Ray Crystallography. By J. Breton (With 4 Figures) | 109 |
| Calculations of Spectroscopic Properties of Bacterial Reaction Centers. By W.W. Parson, A. Scherz, and A. Warshel (With 5 Figures) | 122 |
| On the Temperature-Dependence of the Long Wavelength Fluorescence and Absorption of <i>Rhodopseudomonas viridis</i> Reaction Centers. By P.O.J. Scherer, S.F. Fischer, J.K.H. Hörber, M.E. Michel-Beyerle, and H. Michel (With 3 Figures) | 131 |

| | |
|--|-----|
| Local Environments of Pigments in Reaction Centers of Photosynthetic Bacteria from Resonance Raman Data By M. Lutz and B. Robert (With 4 Figures) | 138 |
| The Spin-Polarization Pattern of the $\Delta m = 1$ Triplet EPR Spectrum of <i>Rps. viridis</i> Reaction Centers By F.G.H. van Wijk, P. Gast, and T.J. Schaafsma | 146 |
| Triplet State Investigation of Charge Separation and Symmetry in Single Crystals of <i>R. viridis</i> Reaction Centers By J.R. Norris, D.E. Budil, H.L. Crespi, M.K. Bowman, P. Gast, C.P. Lin, C.H. Chang, and M. Schiffer | 147 |
| Triplet-minus-Singlet Absorbance Difference Spectroscopy of Photosynthetic Reaction Centers by Absorbance-Detected Magnetic Resonance. By A.J. Hoff (With 11 Figures) | 150 |
| ENDOR Studies of the Primary Donor in Bacterial Reaction Centers. By W. Lubitz, F. Lendzian, M. Plato, K. Möbius, and E. Tränkle (With 6 Figures) | 164 |
| ENDOR of Semiquinones in RCs from <i>Rhodopseudomonas</i> <i>sphaeroides</i> . By G. Feher, R.A. Isaacson, M.Y. Okamura, and W. Lubitz (With 10 Figures) | 174 |
| Photoinduced Charge Separation in Bacterial Reaction Centers Investigated by Triplets and Radical Pairs By J.R. Norris, D.E. Budil, S.V. Kolaczowski, J.H. Tang, and M.K. Bowman (With 5 Figures) | 190 |
| Spin Dipolar Interactions of Radical Pairs in Photosynthetic Reaction Centers. By A. Ogrodnik, W. Lersch, M.E. Michel-Beyerle, J. Deisenhofer, and H. Michel (With 4 Figures) | 198 |
| Protein/Lipid Interaction of Reaction Center and Antenna Proteins. By J. Riegler, W.M. Heckl, J. Peschke, M. Lösche, and H. Möhwald (With 6 Figures) | 207 |
| The Architecture of Photosystem II in Plant Photosynthesis. Which Peptide Subunits Carry the Reaction Center of PS II? By A. Trebst and B. Depka (With 3 Figures) | 216 |

Part III Electron-Transfer: Theory and Model Systems

| | |
|---|-----|
| Application of Electron-Transfer Theory to Several Systems of Biological Interest. By R.A. Marcus and N. Sutin | 226 |
| Effects of Distance, Energy and Molecular Structure on Long- Distance Electron-Transfer Between Molecules By J.R. Miller (With 4 Figures) | 234 |

| | |
|--|-----|
| Ultrafast Electron Transfer in Biomimetic Models of Photosynthetic Reaction Centers. By M.R. Wasielewski, M.P. Niemczyk, W.A. Svec, and E.B. Pewitt (With 5 Figures) | 242 |
| Electron Transfer Through Aromatic Spacers in Bridged Electron-Donor-Acceptor Molecules. By H. Heitele and M.E. Michel-Beyerle | 250 |
| Electron Transfer in Rigidly Linked Donor-Acceptor Systems By S.F. Fischer, I. Nussbaum, and P.O.J. Scherer (With 3 Figures) . | 256 |
| Electron Conduction Along Aliphatic Chains By R. Bittl, H. Treutlein, and K. Schulten (With 4 Figures) | 264 |

Part IV Reaction Centers: Structure and Dynamics

| | |
|--|-----|
| Kinetics and Mechanisms of Initial Electron-Transfer Reactions in <i>Rhodospseudomonas sphaeroides</i> Reaction Centers By W.W. Parson, N.W.T. Woodbury, M. Becker, C. Kirmaier, and D. Holten (With 3 Figures) | 278 |
| Femtosecond Studies of the Reaction Center of <i>Rhodospseudomonas viridis</i> : The Very First Dynamics of the Electron-Transfer Processes. By W. Zinth, M.C. Nuss, M.A. Franz, W. Kaiser, and H. Michel (With 5 Figures) | 286 |
| Analysis of Time-resolved Fluorescence of <i>Rhodospseudomonas viridis</i> Reaction Centers By J.K.H. Hörber, W. Göbel, A. Ogrodnik, M.E. Michel-Beyerle, and E.W. Knapp (With 3 Figures) | 292 |
| The Characterization of the Q _A Binding Site of the Reaction Center of <i>Rhodospseudomonas sphaeroides</i> . By M.R. Gunner, B.S. Braun, J.M. Bruce, and P.L. Dutton (With 2 Figures) | 298 |

**Part V Model Systems on Structure of Antennas
and Reaction Centers**

| | |
|---|-----|
| Structure and Energetics in Reaction Centers and Semi-synthetic Chlorophyll Protein Complexes. By S.G. Boxer (With 4 Figures) .. | 306 |
| Small Oligomers of Bacteriochlorophylls as <i>in vitro</i> Models for the Primary Electron Donors and Light-Harvesting Pigments in Purple Photosynthetic Bacteria By A. Scherz, V. Rosenbach, and S. Malkin (With 7 Figures) | 314 |
| Experimental, Structural and Theoretical Models of Bacteriochlorophylls a, d and g. By J. Fajer, K.M. Barkigia, E. Fujita, D.A. Goff, L.K. Hanson, J.D. Head, T. Horning, K.M. Smith, and M.C. Zerner (With 6 Figures) | 324 |

| | |
|---|------------|
| ENDOR Characterization of Hydrogen-Bonding to Immobilized Quinone Anion Radicals. By P.J. O'Malley, T.K. Chandrashekar, and G.T. Babcock (With 3 Figures) | 339 |
| Concluding Remarks. Some Aspects of Energy Transfer in Antennas and Electron Transfer in Reaction Centers of Photosynthetic Bacteria. By J. Jortner and M.E. Michel-Beyerle (With 6 Figures) | 345 |
| Index of Contributors | 367 |

Picosecond Time-Resolved, Polarized Fluorescence Decay of Phycobilisomes and Constituent Biliproteins Isolated from *Mastigocladus laminosus*

S. Schneider, P. Geiselhart, T. Mindl, and F. Dörr
Institut für Physikalische und Theoretische Chemie,
Technische Universität, D-8046 Garching, F. R. G.

W. John, R. Fischer, and H. Scheer
Botanisches Institut der Universität, D-8000 München 19, F. R. G.

1. Introduction

Phycobiliproteins are photosynthetic light-harvesting pigments in blue-green and red algae. They consist of 2-3 polypeptide subunits, each bearing up to 4 covalently bound linear tetrapyrrolic chromophores [1]. In vivo, the biliproteins are organized into complex structures [2], the phycobilisomes, which are attached to the outer thylakoid surface [3,4]. Energy deposited in the phycobilisomes by light absorption is transferred mainly to photosystem II, which is located in the thylakoid membrane. To achieve efficient energy-transfer, the average excitation energy of the different chromoproteins in the phycobilisomes decreases with decreasing distance to the reaction center. It is generally assumed that the energy-transfer is based upon dipole-dipole-interaction (Förster mechanism). In order to elucidate the importance of the special arrangement of the biliproteins in the phycobilisomes, i.e. the fact that the building blocs of the antenna rods are hexamers, numerous fluorescence studies have been performed on functionally intact phycobilisomes, as well as on their constituent aggregates [4-12]. Apparent differences in the results were blamed on different origin (organism) or preparation procedures, different measuring conditions (low or high light flux with the possibility of non-linear processes), different excitation and observation wavelengths, etc. In this contribution, we summarize our measurements of the fluorescence decay of phycobilisomes from Mastigocladus laminosus and their isolated constituent biliproteins. Special emphasis is thereby given on the additional information, which can be derived from the time-resolved fluorescence polarization. In contrast to earlier measurements [9-12], the excitation wavelength could be chosen down to 545 nm; furthermore, the phycobilisomes of the present mutant were free of phycoerythrocyanin; therefore a possible interference with the decay of this pigment was excluded.

2. Measurements and data analysis

The fluorescence decay curves were measured using a synchronously pumped mode-locked dye laser in conjunction with a repetitively working streak camera (for details see e.g. [11]). The apparent time resolution of this system is approx. 25 ps without deconvolution procedure; it allows measurements with low excitation intensities (10^{13} photons per pulse and cm^2).

From the fluorescence decay curves measured with the analyzer parallel, ($I_{\parallel}(t)$), and orthogonal, ($I_{\perp}(t)$), to the polarization of the exciting beam the expressions $I(t) = I_{\parallel}(t) + 2 \cdot I_{\perp}(t)$ and $D(t) = I_{\parallel}(t) - I_{\perp}(t)$ are calculated. $I(t)$ measures the decay of the excited state population (electronic lifetime) as does a measurement, where the analyzer is set under the magic angle to the excitation polarization. In case of several emitters, their contributions are additive. The difference function $D(t)$ corresponds, in the case of only one kind of emitter, to the product of the excited state population $I(t)$ and the correlation function $C(t)$ of the absorption and emission dipoles (see e.g. [13]). In contrast to the generally discussed anisotropy function $R(t) = D(t)/I(t)$, which for only one emitter represents the correlation function $C(t)$, the difference function $D(t)$ is additive and can therefore be evaluated even if more than one emitting species is present. Furthermore, there are no restrictions with respect to the time resolution of the detection system; quotient formation of convoluted functions $D(t)$ and $I(t)$, resp., would yield erroneous "time-resolved" anisotropy functions $R(t)$ (for more details see e.g. [11] and [14]).

The best fits for both functions (I and D) are determined under the assumption of a bi- or tri-exponential response function by means of a Marquardt algorithm. Depending on the S/N ratio of the recorded fluorescence decay curves and their relative magnitude, the fit parameters derived may be subject to considerable error. Deduction of information on photophysical parameters (lifetimes, fluorescence quantum yields) of phyco-bilisomes or even monomers of biliproteins is impeded by the fact that the total fluorescence is composed of several contributions, namely:

- (i) "leakage" fluorescence from directly excited, energy-transferring chromophors
- (ii) fluorescence from directly excited, terminal chromophors
- (iii) fluorescence from chromophors excited indirectly by energy-transfer, which may or may not transfer their excitation energy to other pigments.

Fluorescence of type (i) and (ii) will rise instantaneously and carry information on the polarization of the exciting light. Fluorescence of the third kind (iii) shows a risetime (negative amplitude in the analysis) and will in general be fairly depolarized due to the randomizing energy-transfer process. In the simple case of a two-component system, the three fluorescence contributions must be superimposed with weighting factors, depending both on the ratio of extinction coefficients at the exciting wavelength and the spectral window of the detection system (fluorescence collection efficiency). One important consequence of this fact is that amplitudes gained from a multi-exponential analysis are without significance unless the weighting factors can be determined sufficiently precisely. E.g., it may happen that in the isotropic fluorescence the rising part of contribution (ii) cancels exactly the fast decaying contribution (i) with the effect that the decay appears essentially as single exponential with the long lifetime of the acceptor chromophor. In the difference function, on the other hand, the decay of the short-lived donor species is easily seen;

its amplitude should be about 0.4 of that of the isotropic contribution of the short-lived donor species, if a random orientational distribution of donor molecules can be assumed. With respect to the amplitude of the short-lived component in a multi-exponential fit, the fraction can be much smaller or larger depending on the extent of compensation discussed above.

In case of rotational relaxation the correlation function $C(t)$ represents a multi-exponential; if the molecule is spherical, $C(t)$ corresponds to a single exponential. Since no better approximations are known, we assume that the correlation function describing the energy-transfer can be approximated by a single exponentially decaying function. Under this circumstance the differences in decay time of the corresponding components of the functions $I(t)$ and $D(t)$, resp. can be associated to depolarizing effects like energy-transfer and orientational relaxation. The latter effect should, however, be without importance in case of protein-bound chromophors (a more detailed discussion will be given elsewhere).

3. Sample Preparation

Mastigocladus laminosus was grown at 52°C in slowly stirred 12 l fermentation flasks in Castenholz medium. Phycobilisomes were isolated by standard procedures [9,10]. The French-pressed cells were first centrifuged at 10,000 g, and the supernatant layered on a sucrose density gradient and spun over night at 140,000 g. Intact phycobilisomes banded in the lower third of the gradient. They had an absorption maximum at 635 nm with a strong shoulder around 620 nm and an emission maximum at 670 nm. Phycoerythrocyanin was isolated from green-light-grown cells following the protocol described for the isolation of phycocyanin [12]. It elutes from DEAE-cellulose column as the first band. The aggregation state was determined by ultracentrifugation from the sedimentation coefficients. The data were analyzed as described earlier [12].

4. Results and Discussion

The isotropic fluorescence decay curves displayed in figure 1a are recorded with 600 nm excitation but different spectral observation windows (cut-off filters). They clearly demonstrate the effect of partial compensation mentioned in chapter 2 onto the amplitude of the short-lived component (see table 1). With a S/N ratio typical for synchroscan streak camera measurements, a tri-exponential fit seems adequate from the point of view of residuals only for trace A; the other two curves (B,C) seem to fit equally well to a biexponential. It should be pointed out that, despite the fact of a rising component in curve C, the onset of the fluorescence in its major part is essentially instantaneous. The difference function $D(t)$ (fig. 1b) can be fit by bi-exponentials with lifetimes of 20 and 1300 ps, resp. The latter value corresponds to the slowest isotropic component, and can be explained by the electronic relaxation of "terminal", immobile chromophors, i.e. the allophycocyanins. Since the amplitude of the "100 ps"- component turns negative for long-wavelength monitoring, it can be assigned to the average energy-transfer time between phycocyanin and allophycocyanin.

Table 1 : Fit parameters derived from the fluorescence decay curves I(t) and D(t) of functionally intact phycobilisomes, isolated from Mastigocladus laminosus, by means of a least square fit procedure.

| Exc.(nm)/Obs.(nm) | T_1 (ps)/A | T_2 (ps)/A | T_3 (ps)/A |
|-------------------|--------------|--------------|--------------|
| 600 >620 | 63 27 | 137 30 | 1342 65 |
| I(t) | >630 | 98 58 | 1346 81 |
| | >645 | 158 13 | 1700 54 |
| | >665 | 100 -7 | 1622 33 |
| | >620 | 20 22 | 1284 4 |
| D(t) | >630 | 23 15 | 1539 5 |
| 580 >590 | 25 29 | 129 16 | 1340 26 |
| I(t) | >600 | 52 20 | 104 31 |
| | >610 | 42 18 | 114 11 |
| D(t) | >590 | 23 10 | 462 30 |
| | >600 | 22 2 | 609 7 |

Because the transferring phycocyanin chromophors are mainly indirectly excited by energy-transfer from the primary absorbers, no additional depolarization is connected with this step.

With 580 nm light, relatively more of the $\beta 2$ -chromophors of phycocyanin are excited (in accordance with [15] the phycocyanobilin bound to cystein 84 of the β -chain is referred to as $\beta 1$ -chromophor, the second, bound to cystein 155 is called $\beta 2$ -chromophor). The isotropic decay curves (fig. 2a) show only decaying components (table 1): the long-lived allophycocyanin emission (~ 1350 ps), an intermediate component (~ 110 ps) and finally a fast component, whose apparent lifetime seems to depend on the observation window. Taking into consideration the parameters derived from the difference function D(t), one may suspect that the shortest component actually represents a mixture with two slightly different lifetimes, one of which is equal to 20 - 25 ps. This lifetime must characterize a very fast decay of directly excited chromophors, i.e. represent the transfer time from α -chromophors, which absorb also at wavelengths around 600 nm. The 50 - 60 ps component would then be related to the deactivation of the $\beta 2$ -chromophors, which, at least in the PC-crystals [15], are located at the perimeter of the trimeric unit. The arrangement of the chromophors in the trimeric units is such that the preferential α - $\beta 1$ energy-transfer is one between neighbouring monomeric units. This fast

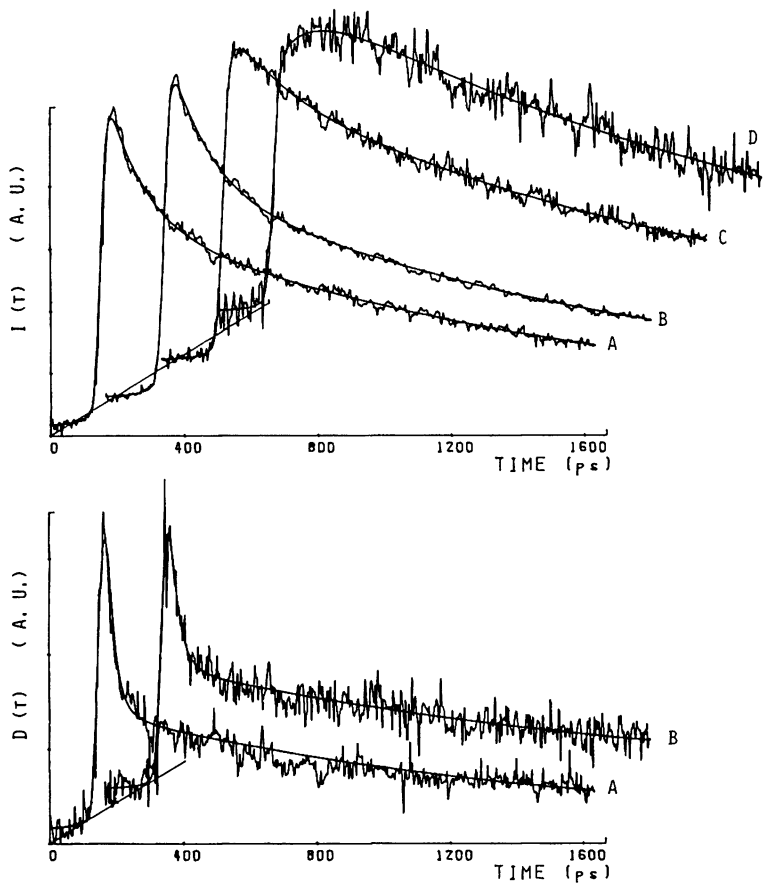


Figure 1: Dependence of fluorescence decay of functionally intact phycobilisomes isolated from *Mastigocladus laminosus* on observation window. Cut-off filters used are: 620 nm (A), 630 nm (B), 645 nm (C) and 665 nm (D). Excitation wavelength in all cases: 600 nm. The parameters of the fit curves are listed in table 1.

transfer route is absent in the monomeric unit and should, according to energetic criteria, be slowed down in phycoerythrocyanin (PEC). In the latter chromoprotein, the α -phycocyanobilin is replaced by a phycoerythrocyanobilin, which absorbs around 568 nm. The deactivation of the β 2-phycocyanobilin must necessarily occur by energy-transfer to the β 1- rather than to the α -chromophor.

In figures 3a and 3b, the functions $I(t)$ and $D(t)$ of PEC-trimers are displayed for various combinations of excitation wavelength and observation window. For long-wavelength excitation (600 nm) the decay is governed by a ~ 350 ps and a ~ 1450 ps component. These values should correspond to the lifetimes of the β 1- (1450 ps) and the β 2- phycocyanobilin (350 ps), resp..

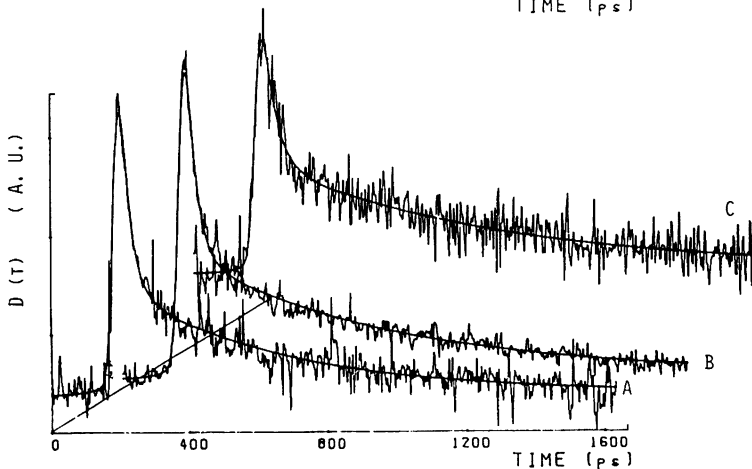
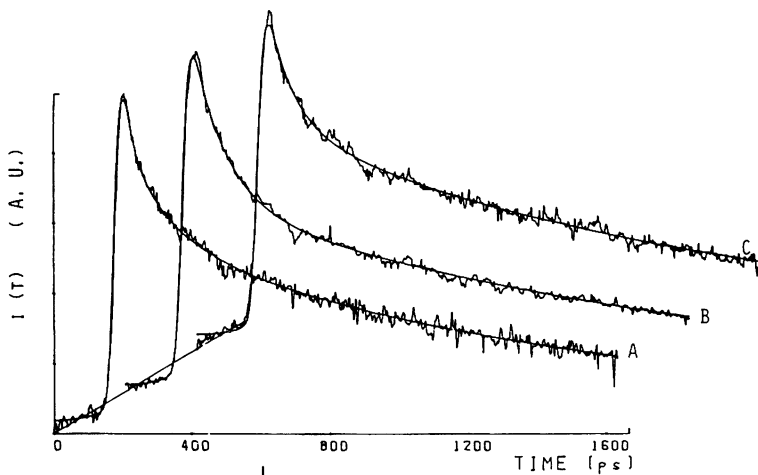


Figure 2: Dependence of fluorescence decay of isolated phycobilisomes on observation window. Cut-off filters used are: 590 nm (A), 600 nm (B), 610 nm (C); excitation wavelength is 580 nm. Fit parameters are listed in table 1.

Decay times of the same magnitude are found in $D(t)$. For 545 nm excitation, a third component is detected both in $I(t)$ and $D(t)$. Its decay time of ~ 110 ps is assigned to the phycoerythrocyanobilin \rightarrow 82- phycocyanobilin transfer time. It should be noted here again that going from 2 to 3-exponential fits, a splitting of one of the components in a faster and a slower one occurs. Therefore, the existence of a certain component must be established by measurements under conditions where that component dominates the decay.

The energetic degeneracy and the therefore possible energy-transfer between like species is, in our opinion, relevant for the interpretation of the decay curves of the trimeric unit

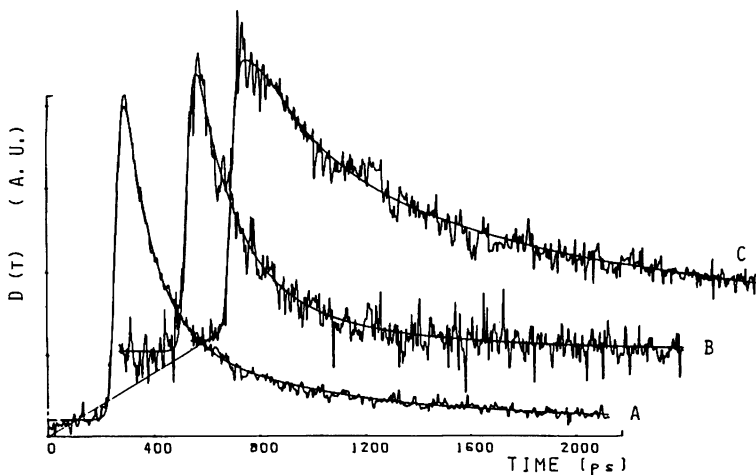
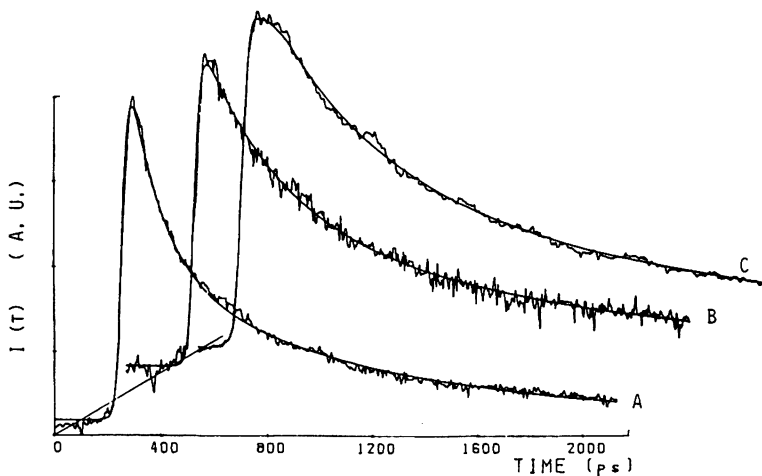


Figure 3: Dependence of fluorescence decay of isolated phycoerythrocyanin on excitation wavelength and observation window, characterized by the cut-off filter. Parameters are $\lambda_{ex} / \lambda_{obs}$ Z_i in ps and A_i in paranthesis.

| | $I(t)$ | $D(t)$ |
|-------------------|-----------------------------|------------------|
| (A) 545nm/ 570nm: | 109(112)/ 470(58)/1500(32) | 106(38)/ 580(13) |
| (B) 545nm/ 590nm: | 270(32)/1400(28) | 144(9)/ 520(3) |
| (C) 600nm/ 610nm: | 370(101)/1500(109) | 260(12)/1530(13) |

shown in figure 4. Under all experimental conditions, the major component is the longest-lived with a decay time of ~ 1400 ps. This value should characterize the "free" decay of the final energy accepting species, the $\beta 1$ -chromophors. The 950 ps-component, which has a counterpart in the $D(t)$ curve, must represent the decay of a rigidly held, but modified species, which is isolated in a sense that energy-transfer to $\beta 1$ -chromophors is prohibited (a similar result and interpretation is given by

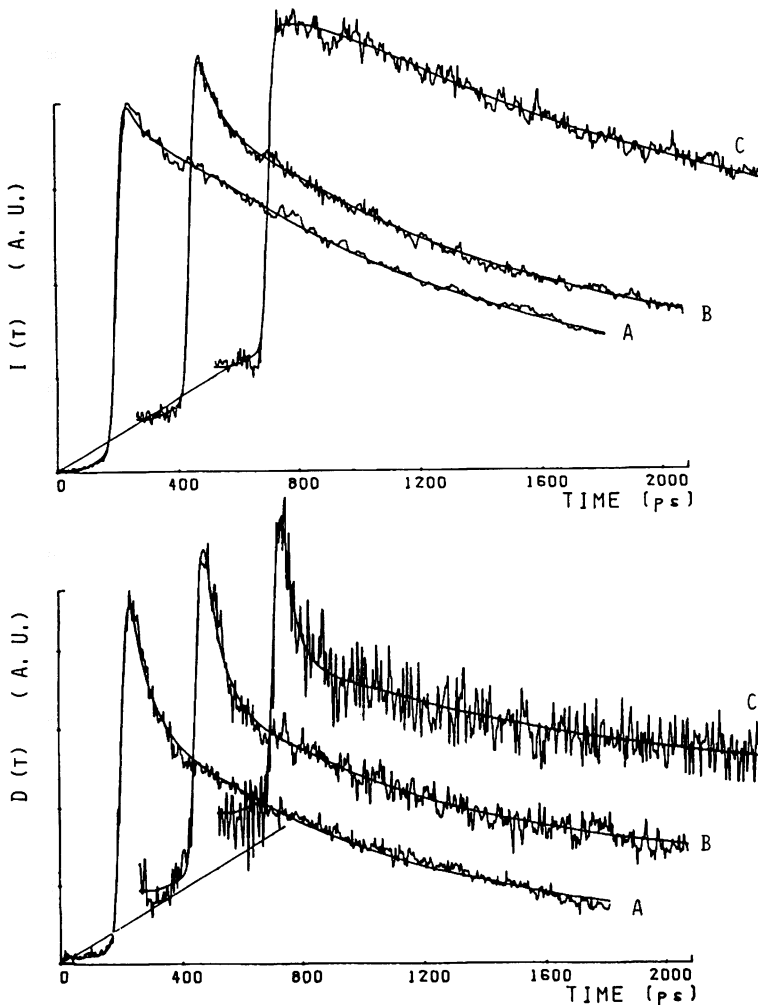


Figure 4: Dependence of fluorescence decay of phycocyanin trimers on excitation wavelength and observation window characterized by the cut-off filter. Parameters are $\lambda_{ex} / \lambda_{obs}$, τ in ps and A; in paranthesis.

| | | |
|-------------------|-----------------------|----------------------|
| (A) 600nm/ 620nm: | I(t):45(47)/1200(190) | D(t):57(41)/ 850(40) |
| (B) 575nm/ 590nm: | I(t):61(77)/1130(150) | D(t):49(43)/ 800(25) |
| (C) 575nm/ 630nm: | I(t):35(1)/1640(80) | D(t):36(18)/1150(8) |

Wendler et al. [16]). Upon short-wavelength excitation and observation the amplitude of the very fast component (40-60 ps) increases. This signals that this component is related to the $\beta 2 \rightarrow \beta 1$ energy-transfer; its value is close to that assigned to this type of transfer in the intact phycobilisomes. In contrast to the latter, the fast 20 ps component, seen mainly in the difference function $D(t)$ is missing in the trimer. The ex-

planation is probably connected to the fact that $\alpha \rightarrow \beta_1$ transfer is no longer irreversible in the trimer, since the energy-difference is of the order of kT only. Lacking the energy drain down the rod by very fast homo-transfer, the energy can circulate among the isoenergetic β_1 -chromophors and eventually be back-transferred to α -chromophors. One may suspect that fluctuations in geometry result in variations of the excitation energy, which are sufficiently large to increase the back- and homo-transfer rates, resp.. For this reason, only energy-transfer from excited β_2 -chromophors would be connected with a significant change of fluorescence polarization.

The above given interpretation could be in contrast to the interaction energies and transfer times derived from crystallographic data [17]. From those it is expected that deactivation of β_2 -chromophors should be dominated by transfer to β_1 -chromophors. The refinement of these data, however, is not yet good enough to give precise information on the complete chromophor structure, and therefore it is not possible to calculate the orientation factors of transition dipole moments and the overlap of donor emission and acceptor absorption spectra.

Acknowledgement. Financial support by Deutsche Forschungsgemeinschaft (SFB 143) and Fonds der Chemie is gratefully acknowledged. We also thank Dr. Hensel and Ms. Renz (München) for the ultracentrifuge measurements.

References

- 1 For a review see e.g.: H. Scheer, in: "Light Reaction Path of Photosynthesis", p. 7, ed. by F.K. Fong (Springer-Verlag, Berlin, 1982)
- 2 E. Mörschel, W. Wehrmeyer: Arch. Microbiol. 113, 83 (1977)
- 3 For a review see e.g.: A.N. Glazer: Ann. Rev. Plant Physiol. 32, 327 (1983)
- 4 For a recent review see e.g.: "Biological events probed by ultrafast laser spectroscopy", ed. by R.R. Alfano (Academic Press, New York, 1982)
- 5 J. Wendler, A.R. Holzwarth, W. Wehrmeyer: Biochim. Biophys. Acta 765, 58 (1984)
- 6 M. Seibert and J.S. Connolly: Photochem. Photobiol. 40, 267 (1984)
- 7 G.W. Suter, P. Mazzola, J. Wendler, A.R. Holzwarth: Biochim. Biophys. Acta 766, 269 (1984)
- 8 W. Haehnel, A.R. Holzwarth, J. Wendler: Photochem. Photobiol. 37, 435 (1983)
- 9 P. Hefferle, M. Nies, W. Wehrmeyer, S. Schneider: Photobiochem. Photobiophys. 5, 41 (1983)
- 10 P. Hefferle, M. Nies, W. Wehrmeyer, S. Schneider: Photobiochem. Photobiophys. 5, 325 (1983)
- 11 P. Hefferle, W. John, H. Scheer, S. Schneider: Photochem. Photobiol. 39, 221 (1984)
- 12 P. Hefferle, P. Geiselhart, T. Mindl, S. Schneider, W. John, H. Scheer: Z. Naturforsch. 39c, 606 (1984)
- 13 G.R. Fleming, J.M. Morris, G.W. Robinson: J. Chem. Phys. 17, 91 (1976)

- 14 J. Papenhuizen and A.J.W.G. Visser: Biophys. Chem. 17, 57 (1983)
- 15 T. Schirmer, W. Bode, R. Huber, W. Sidler, H. Zuber: J. Molecular Biology, submitted; id. in: "Optical Properties and Structure of Tetrapyrroles", ed. by G. Blauer and H. Sund, (Walter de Gruyter, Berlin, 1985)
- 16 J. Wendler, W. John, H. Scheer, A.R. Holzwarth: submitted to Photochem. Photobiol.
- 17 T. Schirmer: PhD-Thesis, TU-München (1985)